ISSN No:-2456-2165

Thermal Radiation, Heat Generation and Soret Effects on Vertical Oscillating Cylinder

G. Palani* and A. Sarojini
Department of Mathematics, Dr. Ambedkar Govt, Arts College
Chennai 600 039, Tamil Nadu, India

Abstract:- An arithmetical methodology is castoff towards study the natural convection with properties of thermal radiation, heat generation and Soret effects on a vertical oscillating cylinder. The governing equations are set up and the resulting equations are changed into a non-dimensional form using the proper non-dimensional quantities. The set of non-dimensional partial differential equations are solved arithmetically using a well-organized method known as Crank-Nicolson method. The velocity, as well as temperature profiles and concentration profiles for different values of parameters taking place into the problem are studied with the assistance of graphs.

Keywords:- *Cylinder, Finite Difference, Heat Generation, Oscillating, Soret Effects.*

I. INTRODUCTION

Convective heat transference stands as one of the most important categories of heat transference and likewise convection is a major kind of mass transference in liquids. Joint hotness as well as mass transference procedure in normal convection captivating the consideration of number of investigators owing to their uses in several twigs of science and engineering. The marvel of natural convective ascends in the liquid what time heat vicissitudes which reason density difference leading to resistance force performing on the liquid elements. This know how to be seen in our routine life in the atmospheric flow which is caused by temperature changes. There are several transportation procedures occurring in environment owed to heat and species concentration changes.

Chen and Yuh [1] studied the steady heat and mass transfer process near cylinders with uniform wall heat and mass fluxes, and wall temperature numerically. Ganesan and Rani [2] premeditated unstable convective movement along a straight up cylinder with collective resistance force effects. Finite-difference process is hired to solve the principal equations approximately. An arithmetical analysis for hotness and concentration driven fleeting free convective nearby a straight up drum was carried out by Rani [3]. The level of temperature and concentration at the cylinder shallow are supposed to fluctuate with exponents *n* and *m* correspondingly in the stream wise coordinate. Approximate outcomes are achieved and exposed with numerous power law changes, thermal as well as mass Grashof numbers. Ganesan and Loganathan [4] inspected transitory natural convective movement of an incompressible liquid along a moving straight up cylinder. They presumed that the heat in addition to absorption of the cylinder exterior remained unvarying. Transitory impact of velocity, temperature as well as concentration sketches are revealed through the assistance of charts.

Heat generation is the energy transported as a result of a divergence in temperature. Heat absorption is the transfer of heat that happens between two bodies, it may occur through by three modes of heat transfer. It is an endothermic reaction so a cooler object absorbs the heat of hotter object. Heat generation/absorptions may be important in weak electrically conducting polymeric liquids due to no change taking place at constant temperature situation and also because of cation and anion salts dissolved in them.

Several procedures in novel engineering regions befall by high temperatures as well as familiarity of radiative heat transference also the convective warmth transference develops an essential for the design of the appropriate paraphernalia. Atomic power plants, fume turbines as well as the numerous driving force devices used for air crafts, arms, satellite broadcasting and interplanetary vehicles are instances of such engineering regions. Furthermore, radiative warmth transference taking place in the liquid intricate know how to be electrically conducting namely ionized owing to extraordinary operative temperature.

Mahfooz *et al*. [5] scrutinized the radiative effects on a transient convective current of optically dense and viscid electrically conducting liquid along a flat surface with heat generation. Sanatan Das *et al* [6] deliberated things of radiations and heat generation on MHD couette movements started exponentially with non-constant wall temperature. Analytical solutions were obtained for the flow problem. Chamkha *et al* [7] tested numerically effects of chemical reaction, Joule-Heating, and thermal emission on MHD unstable natural convective from a porous plate in a micropolar liquid.

The warmth production impact on normal convective movements as well as transmission inside a plumb level plate remains examined. The established controlling equations through the linked boundary environments are rehabilitated to non-dimension forms by means of a local non-similar conversion premeditated by Mamun *et al* [8]. Alam *et al* [9] deliberated numerically for joint free-forced convection and mass transference movement along a plumb permeable level plate, in existence of warmth generation as well as thermal diffusion. Zueco and Ahamed [10] inspected a precise as well as approximate answers of a

stable mixed convective MHD movements of an incompressible viscid electrically conducting liquid along a plumb permeable plate with joint heat and mass transference.

Shariful Alam and Rahman [11] deliberated approximately the problem of a two-dimensional steady MHD convective movement along a permeable plate with Dufour and Soret effects. The numerical values of importance of several parameters entering into the problem gotten then gave a picture graphically. Soret and Dufour impact on hotness and mass transference along a straight up porous cylinder enclosed with Newtonian fluids were inspected by Ching-Yang Cheng [12]. The cubic-spline collaction method are deployed to solve the governing boundary-layer equations. Raju *et al* [13] discussed the effect of magnetic field on natural convection between two heated inclined plates along with Soret effects. Induced magnetic field are neglected in the governing equation then the solution of the resulting equations was obtained by perturbation method. Hence, we propose to study the problem of free convection effects on a semi-infinite vertical oscillating cylinder with thermal radiation, heat source, Soret effects.

II. MATHEMATICAL MODELLING

Contemplate a 2-dimensional viscid incompressible liquid movement along a vertical oscillating cylinder of radius r_0 . At this juncture *x* - axis is selected in the straight up way along the axis of the cylinder as well as the radius coordinates *r* is preferred perpendicular to the cylinder. Furthermore, initially it is supposed that the outer of the cylinder are preserved at the unchanged temperature $T_\infty^{'}$ and the concentration $C_\infty^{'}$ are well-upheld.

As time climbs, the cylinder moves ups and down with the velocity $u_o \cos \omega' t'$ in the straight up way. The temperature and concentration on the cylinder surface are also raised to $T_w^{'}$ and $C_w^{'}$. We abandonment the viscous dissipative effects in the temperature equation.

The liquid possessions are taken to be unvarying and take exemption to density divergence which inspire pertness strength term in the velocity equation and it ploy key factor the discussion. We can study the impacts of the equations which governs continuity, compelling force or strength and a thermodynamic quantity equivalent to the capacity of a physical system to do

$$\frac{\partial (ru)}{\partial x}+\frac{\partial (rv)}{\partial r}=0 \tag{1}$$

$$\frac{\partial u}{\partial t'}+u\frac{\partial u}{\partial x}+v\frac{\partial u}{\partial r}=g\beta (T'-T_\infty')+g\beta^{*}(C'-C_\infty')+\frac{v}{r}\frac{\partial}{\partial r}\left(r\frac{\partial u}{\partial r}\right) \tag{2}$$

$$\frac{\partial T'}{\partial t'}+u\frac{\partial T'}{\partial x}+v\frac{\partial T'}{\partial r}=\frac{\alpha}{r}\frac{\partial}{\partial r}\left(r\frac{\partial T'}{\partial r}\right)+\frac{Q_0}{\rho C_\rho}(T'-T_\infty')-\frac{1}{\rho C_\rho}\frac{\partial}{\partial r}(rq_r) \tag{3}$$

$$\frac{\partial C'}{\partial t'}+u\frac{\partial C'}{\partial x}+v\frac{\partial C'}{\partial r}=\frac{D}{r}\frac{\partial}{\partial r}\left(r\frac{\partial C'}{\partial r}\right)+\frac{DK_T}{T_m'}\frac{1}{r}\frac{\partial}{\partial r}\left(r\frac{\partial T'}{\partial r}\right) \tag{4}$$

The radiative heat flux term *i.e.*, $\frac{\partial q_r}{\partial r}$ in the energy equation is simplified by utilizing the Rosseland approximation (Brewster [14]) as follows,

$$q_r=\frac{-4\sigma^{*}}{3k^{*}}\frac{\partial T'^{4}}{\partial r} \tag{5}$$

It must be perceived that by exhausting the Rosseland approximation we restrict our investigation to optically dense liquids. If temperatures variances $T'-T_\infty'$ inside the flow are adequately insignificant at that moment equation (5) can be linearized by T'^{4} into the Taylor series near by T_∞' which subsequently abandoning higher order terms takes the form

$$T'^{4}\cong 4T_\infty'^{3}T'-3T_\infty'^{4} \tag{6}$$

Consuming equations (5) and (6) in (3) contributes

$$\frac{\partial T'}{\partial t'}+u\frac{\partial T'}{\partial x}+v\frac{\partial T'}{\partial r}=\frac{k}{\rho C_\rho}\frac{1}{r}\frac{\partial}{\partial r}\left(r\frac{\partial T'}{\partial r}\right)+\frac{Q_0}{\rho C_\rho}(T'-T_\infty')+\frac{16\sigma^{*}T_\infty'^{3}}{3k^{*}\rho C_\rho}\frac{1}{r}\frac{\partial (rq_r)}{\partial r} \tag{7}$$

The initial and boundary conditions are

$$\begin{aligned}
&t'\le 0: \quad u=0, \quad v=0, \quad T'=T_\infty', \quad C'=C_\infty' \quad \text{for all } x \text{ and } r\ge r_0\\
&t'>0: \quad u=u_0\cos\omega' t', \quad v=0, \quad T'=T_w', \quad C'=C_w' \quad \text{at } r=r_0\\
&\qquad\quad u=0 \qquad\qquad\quad T'=T_\infty', \quad C'=C_\infty' \quad \text{at } x=0 \text{ and } r\ge r_0\\
&\qquad\quad u\to 0, \qquad\qquad T'\to T_\infty', \quad C'\to C_\infty' \quad \text{as } r\to\infty
\end{aligned} \tag{8}$$

The local values of shear stress, heat transference rate number and Sherwood number are given below:

$$\tau_x = -\mu\left(\frac{\partial u}{\partial r}\right)_{r=r_0} \tag{9}$$

$$Nu_x = \frac{x}{T'_\omega - T'_\infty}\left(-\frac{\partial T'}{\partial r}\right)_{r=r_0} \tag{10}$$

$$Sh_x = \frac{x}{C'_w - C'_\infty}\left(-\frac{\partial C'}{\partial r}\right)_{r=r_0} \tag{11}$$

The time reliance values of shear stress, heat transference rate number and Sherwood number are given underneath:

$$\overline{\tau}_L = \frac{1}{L}\int_0^L \mu\left(\frac{\partial u}{\partial r}\right)_{r=r_0} dx \tag{12}$$

$$\overline{Nu_L} = \int_0^L \frac{1}{T'_\omega - T'_\infty}\left(-\frac{\partial T'}{\partial r}\right)_{r=r_0} dx \tag{13}$$

$$\overline{Sh_L} = \int_0^L \frac{1}{C'_w - C'_\infty}\left(-\frac{\partial C'}{\partial r}\right)_{r=r_0} dx \tag{14}$$

Using the ensuing non-dimensional quantities:

$$X = \frac{xv}{u_0 r_0^2},\ R = \frac{r}{r_0},\ U = \frac{u}{u_0},\ V = \frac{vr_0}{v},\ t = \frac{vt'}{r_0^2}, T = \frac{T' - T'_\infty}{T'_w - T'_\infty},$$

$$C = \frac{C' - C'_\infty}{C'_w - C'_\infty},\ Gr = \frac{g\beta\left(T'_w - T'_\infty\right)r_0^2}{vu_0},\ Gc = \frac{g\beta\left(C'_w - C'_\infty\right)r_0^2}{vu_0} \tag{15}$$

$$\Pr = \frac{\mu C_p}{k},\ S_r = \frac{D_m K_T\left(T'_w - T'_\infty\right)}{vT'_m\left(C'_w - C'_\infty\right)}, \phi = \frac{Q_0 r_0^2}{\mu C_p},\ \omega = \frac{r_0^2\omega'}{v},\ N = \frac{k^* k}{4\sigma T'^3_\infty}$$

Equations (1), (2), (7) and (4) are compressed to the succeeding dimensionless form:

$$\frac{\partial U}{\partial X} + \frac{\partial V}{\partial R} + \frac{V}{R} = 0 \tag{16}$$

$$\frac{\partial U}{\partial t} + U\frac{\partial U}{\partial X} + V\frac{\partial U}{\partial R} = GrT + GcC\frac{1}{R}\frac{\partial}{\partial R}\left(R\frac{\partial U}{\partial R}\right) \tag{17}$$

$$\frac{\partial T}{\partial t} + U\frac{\partial T}{\partial X} + V\frac{\partial T}{\partial R} = \frac{1}{\Pr}\left(\frac{3N+4}{3N}\right)\frac{1}{R}\frac{\partial}{\partial R}\left(R\frac{\partial T}{\partial R}\right) + \phi T \tag{18}$$

$$\frac{\partial C}{\partial t} + U\frac{\partial C}{\partial X} + V\frac{\partial C}{\partial R} = \frac{1}{Sc}\frac{1}{R}\frac{\partial}{\partial R}\left(R\frac{\partial C}{\partial R}\right) + S_r\frac{1}{R}\frac{\partial}{\partial R}\left(R\frac{\partial T}{\partial R}\right) \tag{19}$$

The corresponding dimensionless initial and boundary situations are:

$$\begin{aligned}
&t \le 0: && U = 0, && V = 0, && T = 0, C = 0 && \text{for all } X \text{ and } R\\
&t > 0: && U = \cos\omega t, && V = 0, && T = 1, C = 1 && \text{at } R = 1\\
& && U = 0 && T = 0, && C = 0 && \text{at } X = 0\\
& && U \to 0, && T \to 0, && C \to 0 && \text{as } R \to \infty
\end{aligned} \tag{20}$$

The local shearing stress, rate of heat transference as well as rate of mass transference in non-dimensional form:

$$\tau_X = -\left(\frac{\partial U}{\partial R}\right)_{R=1} \tag{21}$$

$$Nu_X = \frac{-X\left(\frac{\partial T}{\partial R}\right)_{R=1}}{T_{R=1}}, \tag{22}$$

$$Sh_X = \frac{-X\left(\frac{\partial C}{\partial R}\right)_{R=1}}{C_{R=1}}, \tag{23}$$

Dimensionless form of the average shearing stress, rate of heat transference as well as rate of mass transference are:

$$\overline{\tau} = -\int_0^1 X\left(\frac{\partial U}{\partial R}\right)_{R=1} dX \tag{24}$$

$$\overline{Nu} = -\int_0^1 \frac{\left(\frac{\partial T}{\partial R}\right)_{R=1}}{T_{R=1}} dX \tag{25}$$

$$\overline{Sh} = -\int_0^1 \frac{\left(\frac{\partial C}{\partial R}\right)_{R=1}}{C_{R=1}} dX \tag{26}$$

III. COMPUTATIONAL PROCEDURES

The transient, non-linear coupled PDEs (16)-(19) with (20) are worked out by using Crank-Nicholson method. The integral area is considered oblong with edges X_{max}(= 1) and R_{max}(=19). The value of R_{max} be companionable to $R = \infty$, it is located exterior to the velocity and temperature boundary layers. The extreme of *R* was picked as 21 when roughly primary inquiries were carried out subsequently the latter two of the boundary conditions (20) remain fulfilled.

To get a reasonable and consistent mesh scheme for the calculations, a grid individuality is executed. Henceforth the mesh scheme of 50 x 105 remains nominated for entirely ensuing analysis by way of ΔX = 0.02 and ΔR = 0.2.

Besides the time-pace dimension dependence is implemented, which produces Δt = 0.01 for consistent outcomes. Henceforth, the overhead cited sizes have been measured as suitable mesh sizes for calculation. Calculations remain worked out until the stable state is touched. The stable state answer is presumed to have been touched, at what time the absolute variance among the quantities of U, T as well as temperature C at two succeeding iterations are fewer than 10^{-5} at all meshes.

The derivatives intricate in equations (21)-(26) are assessed by means of a five point approximation formula, after that Newton-Cotes closed integration formula used to evaluate integrals.

IV. DISCUSSION OF FALL OUTS

The acquired outcomes remain linked with the accessible fallouts in the works of Chen and Yuh [1] for $\Pr = 0.7$, $Sc = 0.2$, $Gc = 2.0$ and $Gr = 1.0$. An outstanding agreement is experiential in the evaluation.

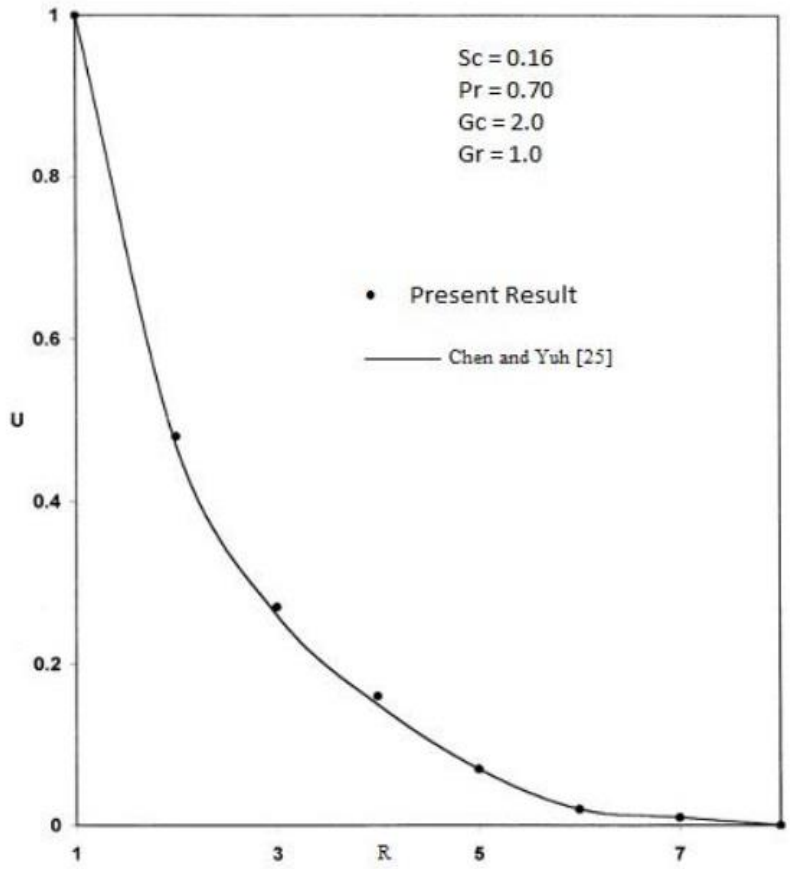

Figure 1 Comparison of temperature outlines

The transitory velocity, temperature as well as concentration silhouettes used for dissimilar quantities of *Gr* and *Gc* at the foremost verge remain exhibited graphically in the Figures 2 to 4 correspondingly. The situation is experiential that the liquid swiftness growths gradually by way of time which touches the time-based maximum and then consequently the situation reaches the stable position. Velocity upsurges as thermal Grashof number Gr or mass Grashof number *Gc* rises. The involvement of mass dispersion to the resistance strength upsurges the extreme velocity considerably. The arithmetical values demonstrate that there is a decline in the temperature for greater values of *Gr* or *Gc*. The time-based maximum temperature experiential in Figure 3. Similarly, we perceived that the concentration upsurges by way of diminishing value of *Gr* and *Gc*.

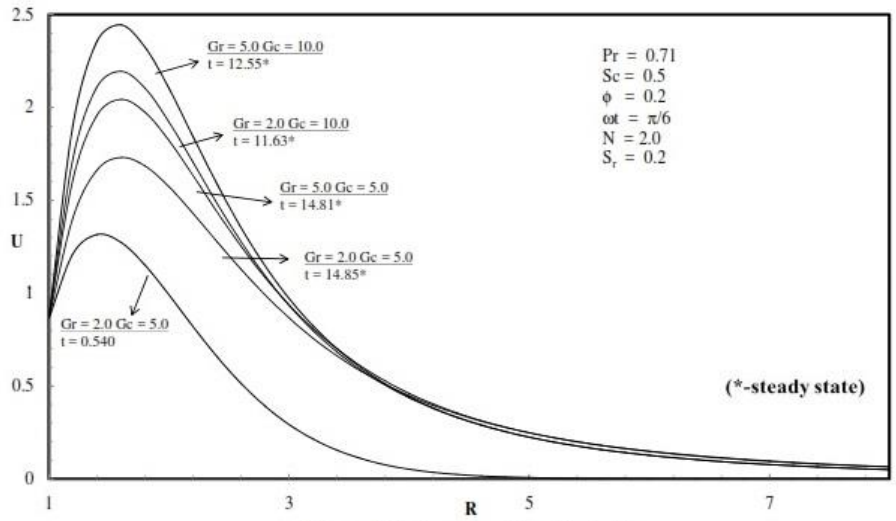

Figure 2 Unsteady outline of velocity in numerous values of Gr and Gc

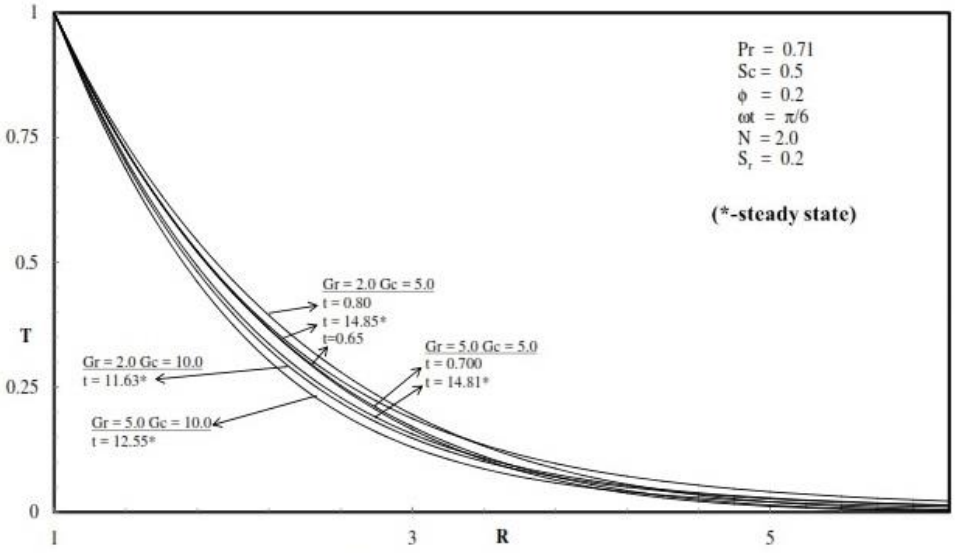

Figure 3 Unsteady outline of temparture in numerous values of Gr and Gc

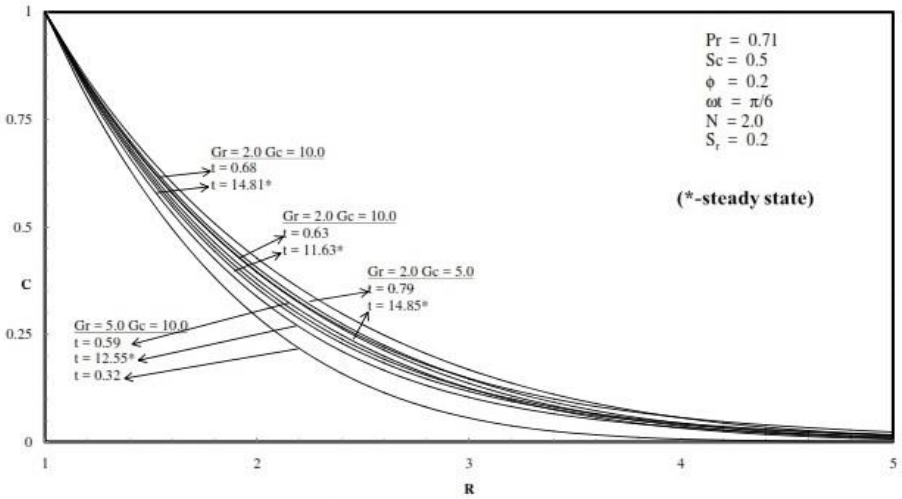

Figure 4 Unsteady outline of Concentration in numerous values of Gr and Gc

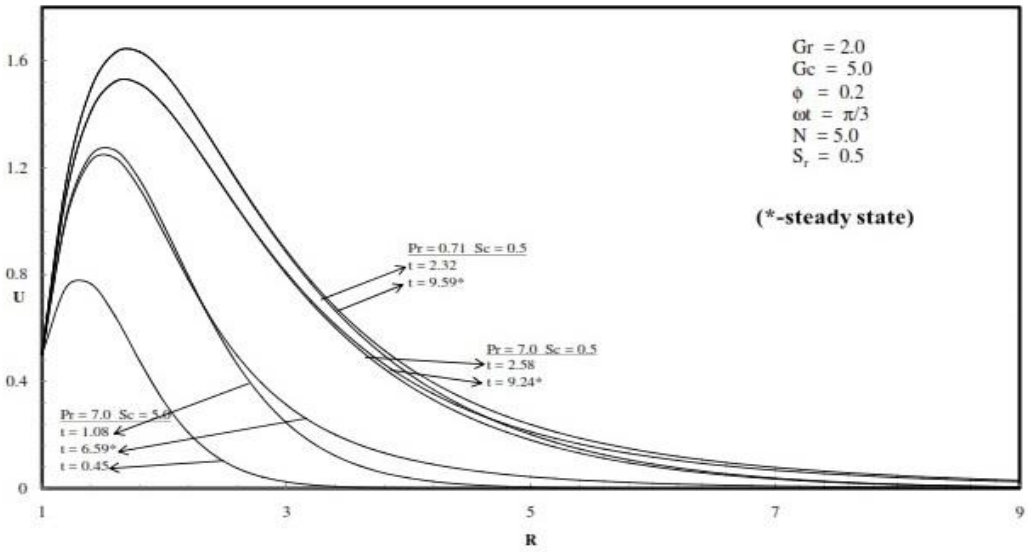

Figure 5 Unsteady outline of velocity in numerous values of Pr and Sc

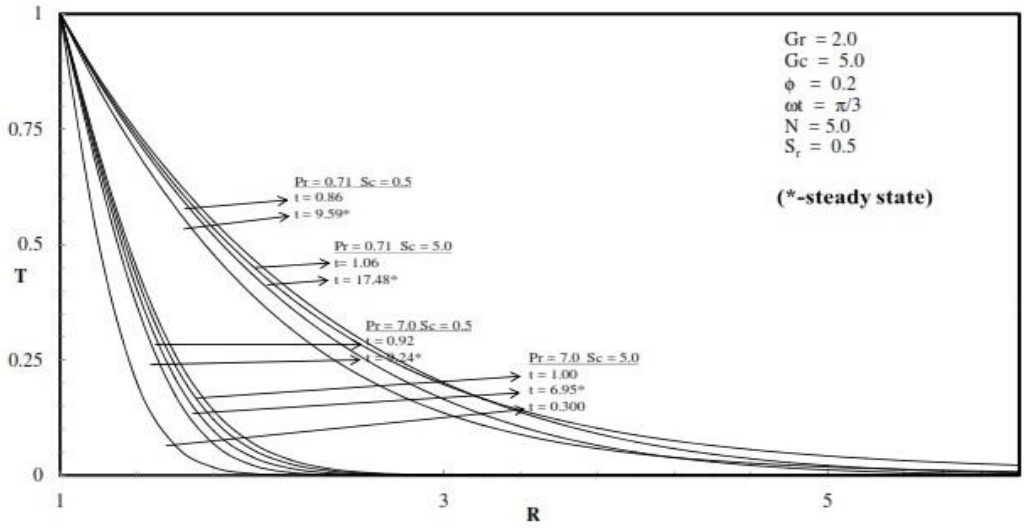

Figure 6 Unsteady outline of temperature in numerous values of Pr and Sc

Figures 5 to 7, exclusively displays that the dissimilarity of *Pr* and *Sc* on velocity, temperature and concentration. As of the Figure 5, we grasp that the velocity upsurges significantly neighboring the cylinder surface then falloffs progressively away from the cylindrical surface. The lesser value of *Sc* is characterized such as lighter fume while the greater value of Sc characterized is as heavier fume. Furthermore, we witnessed that the lighter fume velocity is over and above that of heavier fumes. Time obligatory to touch the stable position upsurges in place of greater values of *Pr*. The variance among the time-based maximum as well as stable position escalates as the value of Sc rises. The temperature silhouettes diminution with reducing value of *Sc* and rises by way of reducing value of *Pr*. The impact of *Pr* remains more significant in the temperature silhouette than the other factors. From the Figure 7, we perceived that the species concentration silhouettes upsurge with diminishing value of *Sc*, on the other hand the aforementioned rises with growing value of *Pr*.

Transitory velocity, temperature as well as concentration outlines at the foremost verge of the cylinder surface for several values of thermal radiation parameter N and heat source parameter ϕ are revealed graphically in Figures 8-10. Time obligatory to touch the stable position upsurges as ϕ drops where as this one intensification as radiative factor upturns.

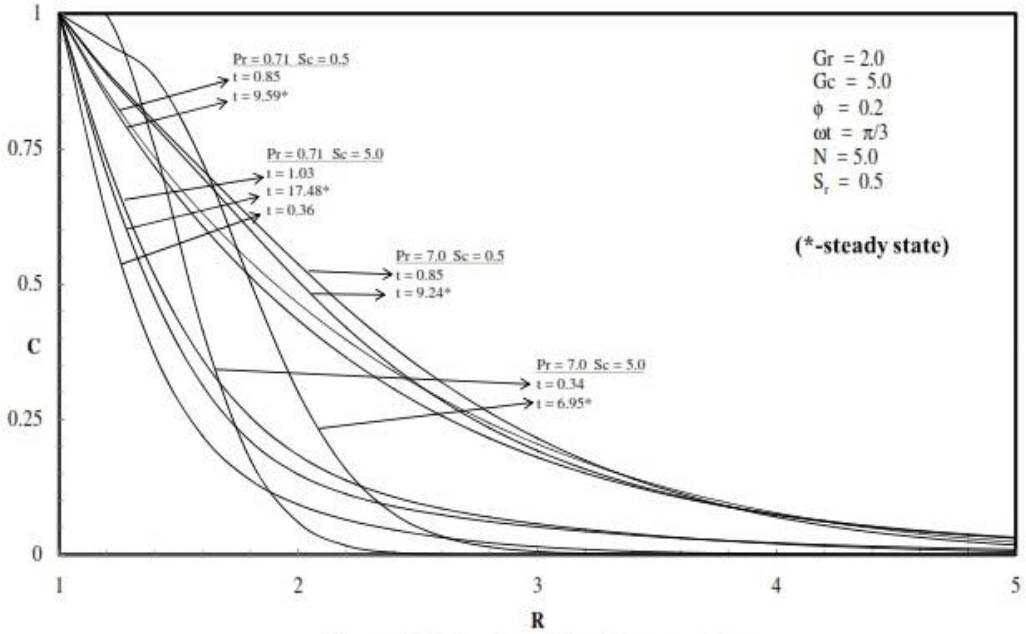

Figure 7 Unsteady outline of concentration in numerous values of Pr and Sc

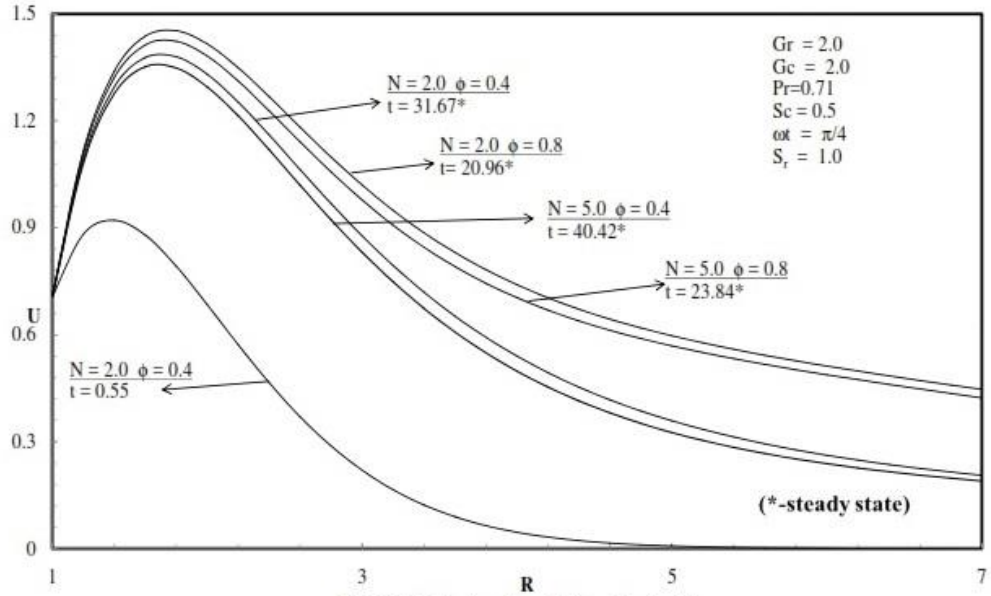

Figure 8 Unsteady outline of velocity in numerous values of N and ϕ

Figure 8 demonstrates that the air swiftness upturns as the radiative factor rises. Owing to the existence of heat source dynamism, the air velocity has grown. This one is got that the temperature growths as *N* rises. This consequence reaches a decision by way of anticipations, meanwhile the impact of radioactivity and shallow temperature remains to upsurge the energy transport rate of the liquid, in this manner, thus growing the liquid temperature.

The situation is detected that the stint obligatory to touch the stable position growths by means of the growing value of radiative factor *N*, this indicates that the presence of radioactivity assistances to accomplish the stable position gradually. The existence of a heat source in the boundary layer engenders energy, which starts the liquid temperature upturn. Similarly, it is witnessed that growing value of *N* relates to a denser concentration comparative to the momentum boundary layer.

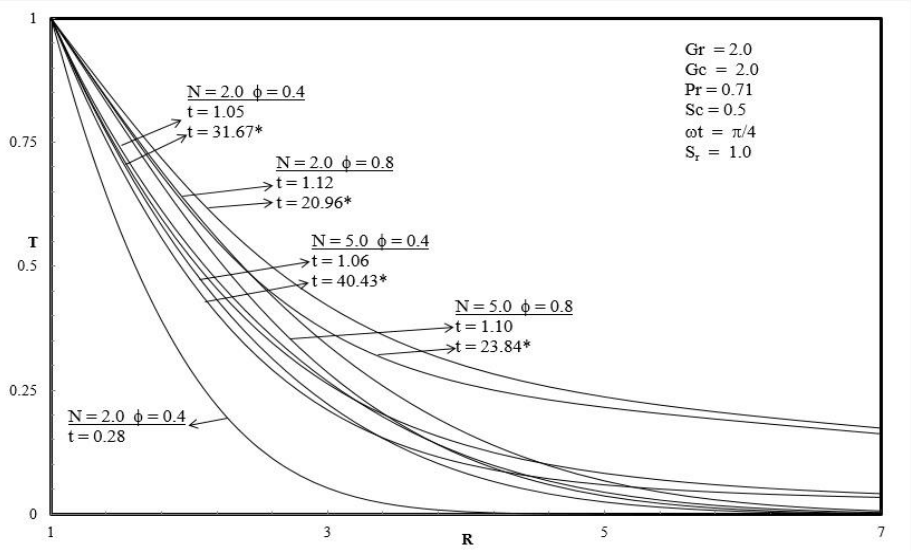

Figure 9 Transient temperature profiles at X=1.0 for different N and ϕ (*-steady state)

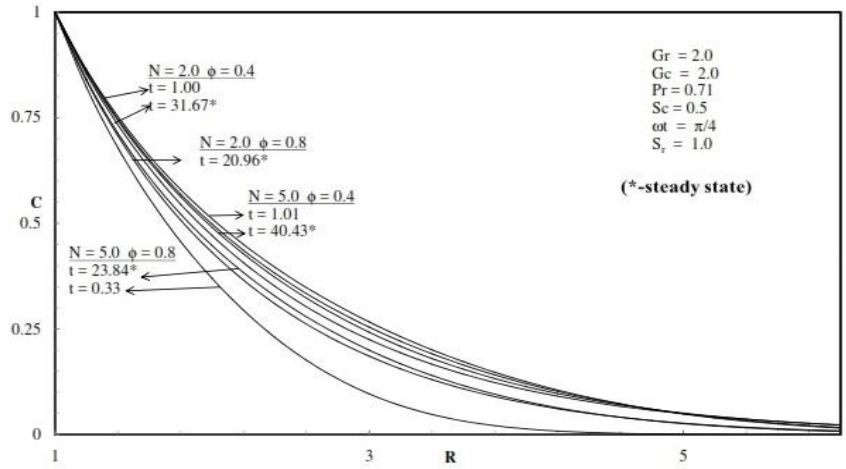

Figure 10 Unsteady outline of concentration in numerous values of N and ϕ

Time-based maximum and stable position values for dissimilar quantity of oscillation factor ωt and Soret S_r for velocity, temperature and concentration shapes at the foremost verge of the cylinder are displayed in Figures 11-13. This one is experiential that velocity upsurges with growing value of phase angle ωt .

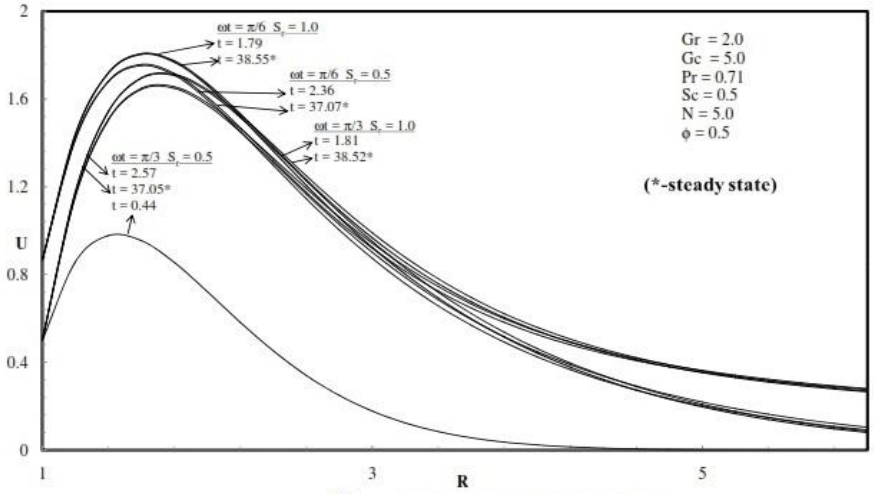

Figure 11 Unsteady outline of velocity in numerous values of ωt and S_r

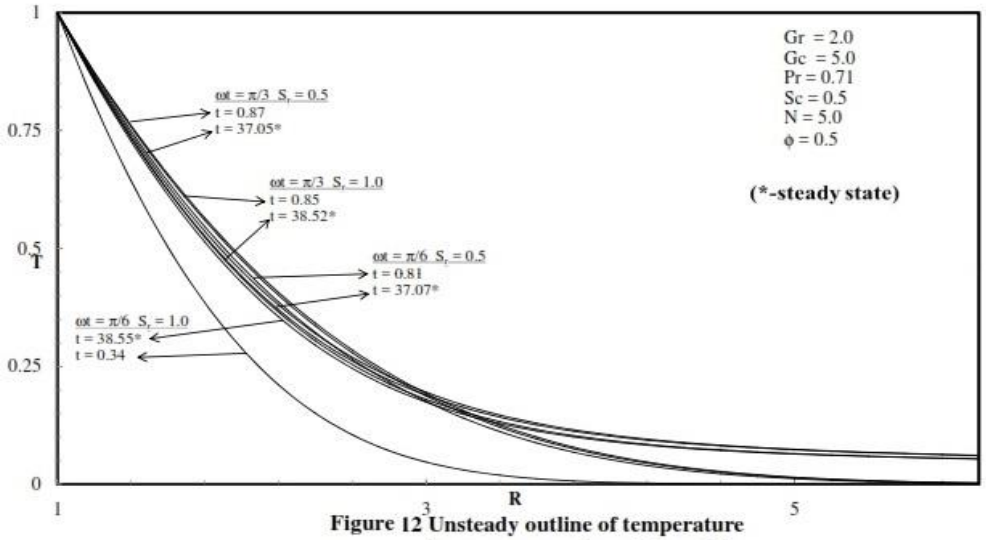

Figure 12 Unsteady outline of temperature in numerous values of ωt and S_r

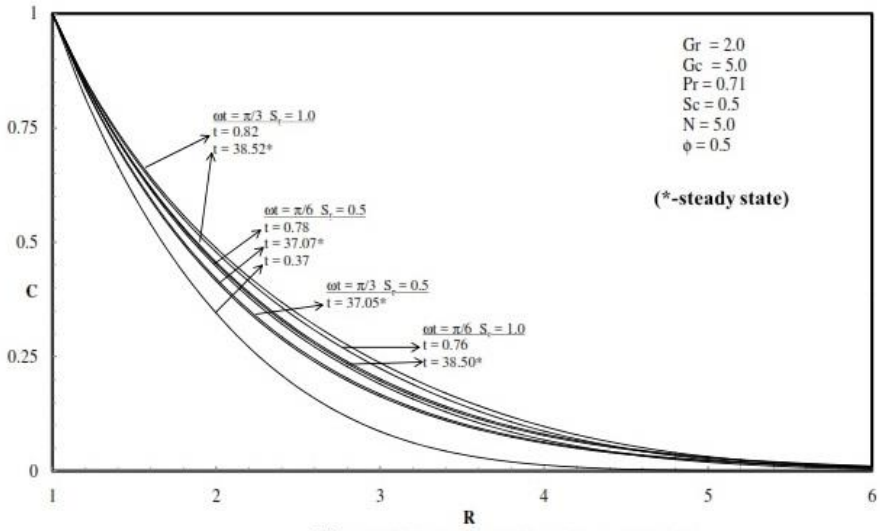

Figure 13 Unsteady outline of concentration in numerous values of ωt and S_r

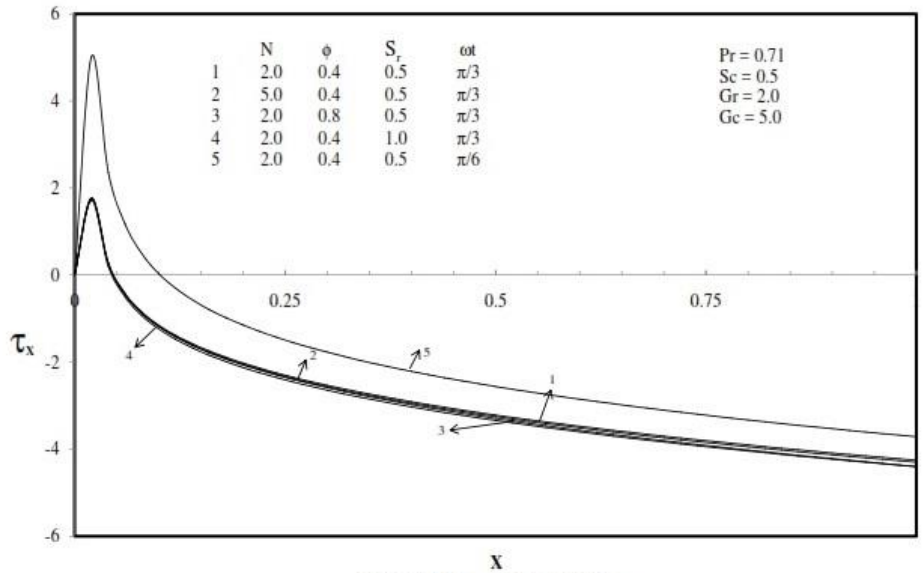

Figure 14 Local skin friction

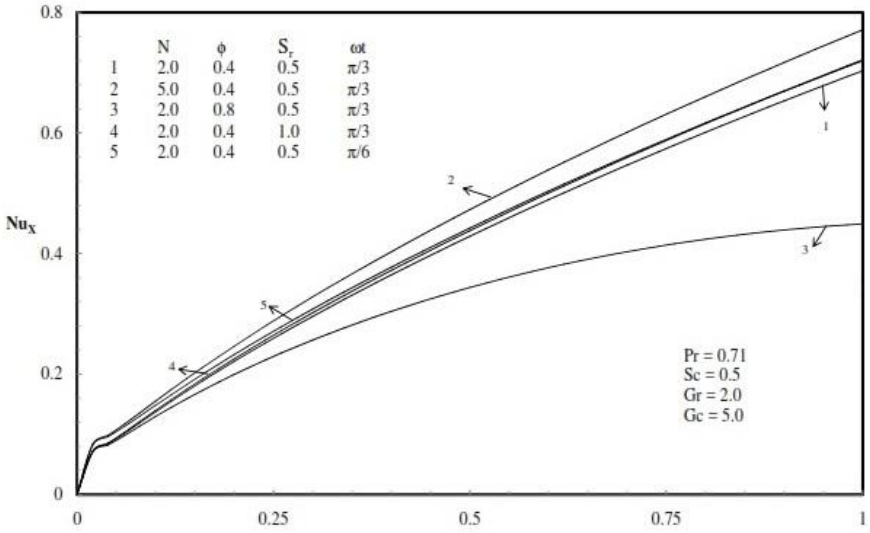

Figure 15 Local Nusselt number

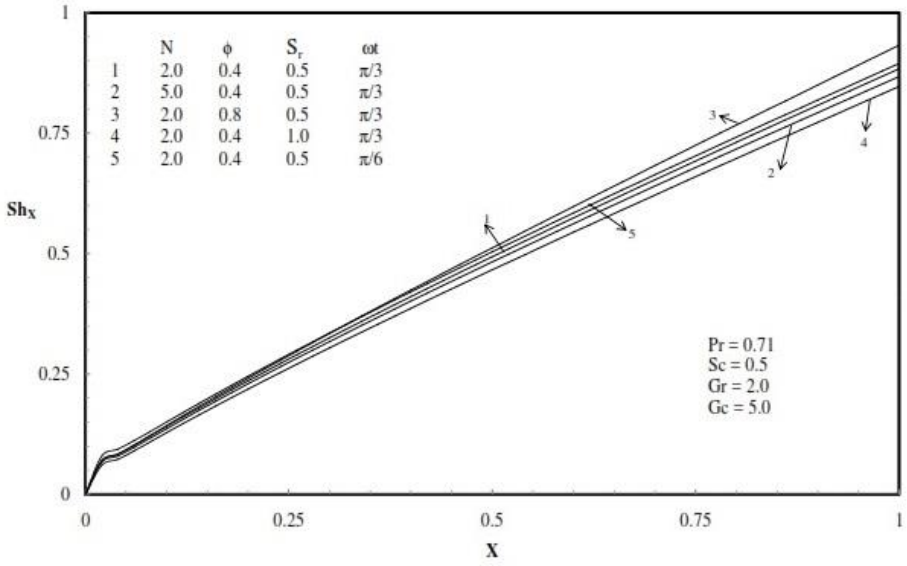

Figure 16 Local Sherwood number

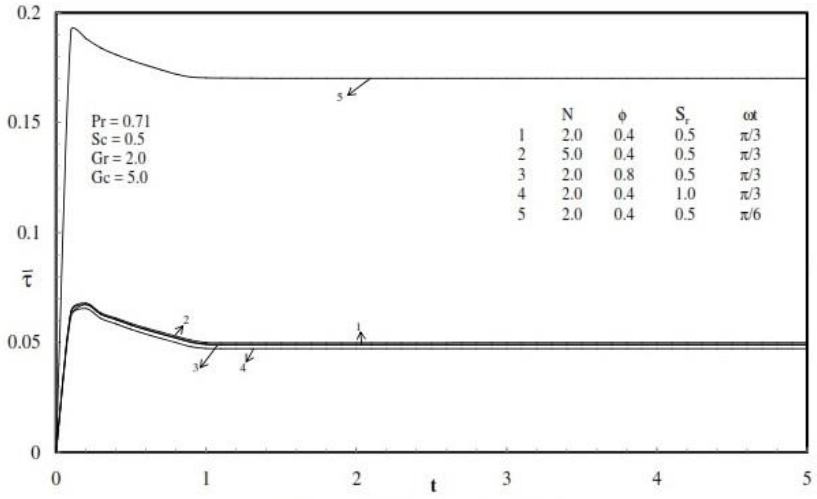

Figure 17 Average skin friction

Additional stint is necessary to touch the stable position in the event of phase angle $\omega t = 0$. The velocity and concentration escalates, on the other hand, the temperature drops through growing value of Soret. This performance remains a straight significance of the Soret impact, which yields a mass change from lesser towards greater solute concentration controlled by the temperature gradient. Likewise, at the time where S_r is adequately high, the heat and the solute resistance forces combine their activities to improve the convection, which leads to the upsurge in the liquid swiftness. The Soret number takes significant impact on the temperature and concentration in association with the velocity.

An estimated quantities of stable position shear stress, Nusselt number and Sherwood number are premeditated then exposed sketchily in the Figures 14-16 respectively. The shearing stress falls as ωt nurtures. The situation is witnessed that rate of heat transference declines as ωt growths. Likewise, the rate of mass transference diminutions as ωt increases.

Average values of shear stress, Nusselt number and Sherwood number are revealed graphically in Figures 17-19 in that order at X=1.0. The situation stays remarked that average shear stress diminutions, as ωt upturns throughout the transitory retro. The average Nusselt number diminishes as ωt rises. In the same way, the average Sherwood number diminishes as ωt rises.

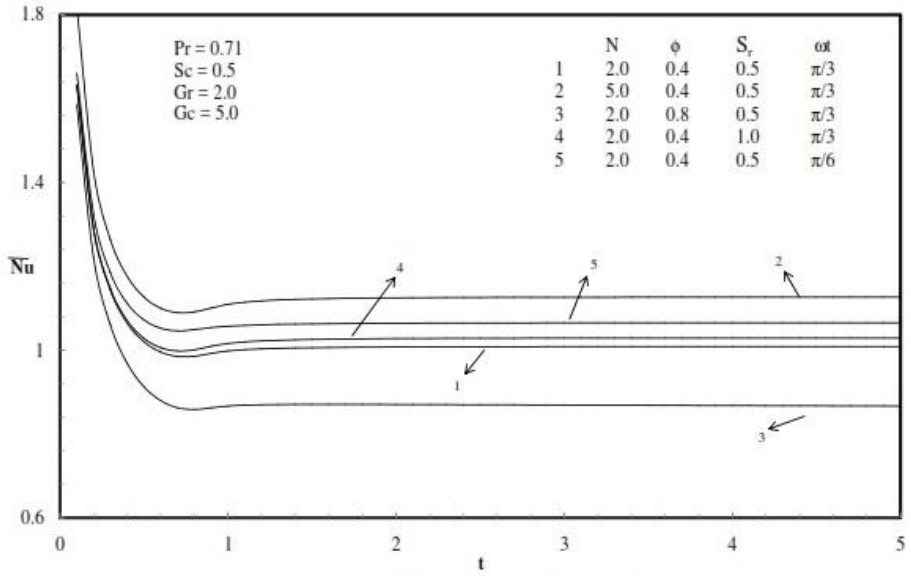

Figure 18 Average Nusselt number

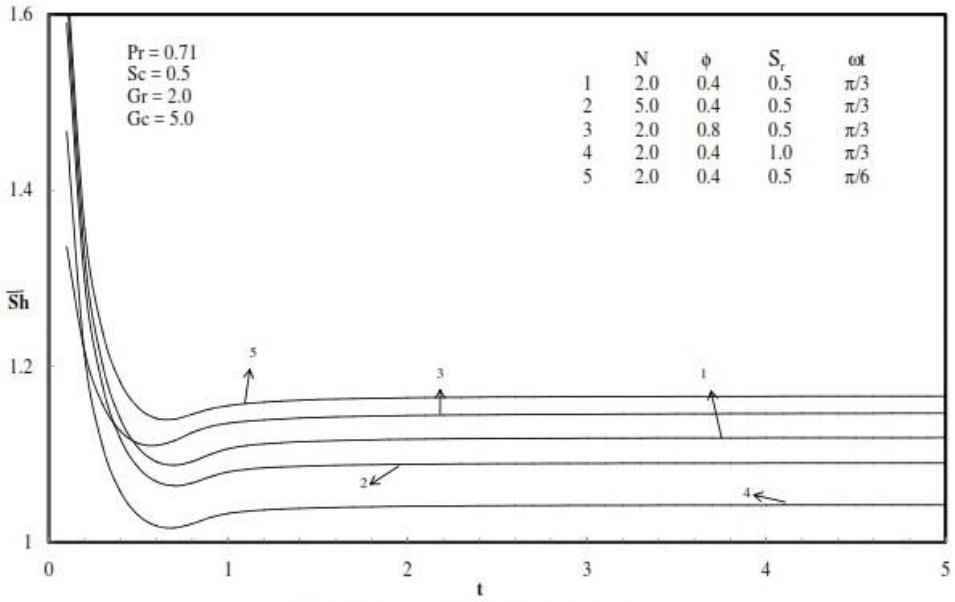

Figure 19 Average Sherwood number

V. CONCLUDING REMARKS

Thermal radiation, heat source as well as Soret effects impacting on convective currents along a semi-infinite plumb oscillating cylinder remains deliberated. Crank-Nicholson kind of implied finite difference process was betrothed to solve the non-dimensional controlling equations. From the arithmetical outcomes, the ensuing inferences are drawn:

- The situation is experiential that the liquid swiftness grows gradually by way of time as it touches the time-based maximum and then consequently the situation reaches the stable position.
- The arithmetical values demonstrate that there is a decline in the temperature for greater values of Gr or Gc.
- The velocity and concentration escalates, on the other hand the temperature drops through growing value of Soret.
- The rate of mass transference diminutions as ωt increases.
- The average Nusselt number diminishes as ωt rises.

REFERENCES

[1]. Chen T.S., and Yuh C.F., Combined Heat and Mass Transfer in Natural Convection along a vertical cylinder, International Journal of Heat Mass Transfer, 23, 451-461, 1980.
[2]. Ganesan P., and Rani H.P., Transient natural convection flow over a vertical cylinder with variable surface temperatures, Forschung im Ingenierwesen, 66, 11-16,2000.
[3]. Rani H.P., Transient natural convection along a vertical cylinder with variable surface temperature and mass diffusion, Heat and Mass Transfer, 40, 67-73, 2003.
[4]. Ganesan P., and Loganathan P., Unsteady natural convective flow past a moving vertical cylinder with heat and mass transfer, Heat and Mass Transfer, 37, 59-65, 2001.
[5]. Mahfooz S.M., Hossain M.A., and Gorla R.S.R., Radiation effects on transient magneto hydrodynamic natural convection flow with heat generation, International Journal of Thermal Sciences, 58, 79-91, 2012.
[6]. Das S., Sarkar B.C., and Jana R.N., Radiation effects on free convection MHD couette flow started exponentially with variable wall temperature in presence of heat generation, Open Journal of Fluid Dynamics, 2, 14-27, 2012.
[7]. Chamkha A.J., Mohamed R.A., and Ahmed S.E., Unsteady MHD natural convection from a heated vertical porous plate in a micropolar fluid with joule heating, chemical reaction and radiation effects, Meccanica, 46, 399-411, 2011.
[8]. Mamun A.A., Chowdhury Z.R., Azim M.A., and Maleque M.A., Conjugate heat transfer for a vertical flat plate with heat generation effect. Nonlinear Analysis: Modelling and Control, 13(2), 213-223, 2008.
[9]. Alam M.S., Rahman M.M., and Samad M.A., Numerical study of the combined free-forced convection and mass transfer flow past a vertical porous plate in a porous medium with heat generation and thermal diffusion, Non-liner Analysis: Modelling and Control, 11(4), 331-343, 2006.
[10]. Zueco J., and Ahmed S., Combined heat and mass transfer by mixed convection MHD flow along a porous plate with chemical reaction in presence of heat source, Applied Mathematics and Mechanics, 31(10), 1217-1230, 2010.
[11]. Mohamed Shariful Alam and Mohammad Mansur Rahman., Dufour and Soret effects on MHD free convective heat and mass transfer flow past a vertical porous flat plate embedded in a porous medium, Journal of Naval Architecture and Marine Engineering, 53-65, June 2005.
[12]. Ching-Yang Cheng., Soret and Dufour effects on free convection boundary layer over a vertical cylinder in a saturated porous medium, International Communications in Heat and Mass Transfer, 37, 796-800, 2010.
[13]. Raju M.C., Varma S.V.K., Reddy P.V., and Sumon Saha., Soret effects due to natural convection between heated inclined plates with magnetic field, Journal of Mechanical Engineering, ME: 39 (2), 65-70, 2008.
[14]. Brewster M.Q., Thermal Radiative Transfer and Properties, New York, John Wiley and Sons, Inc, 1992.
[15]. Carnahan B., Luther H.A. and Wilkes J.O., Applied Numerical Methods, John Wiley and Sons, New York, 1969.